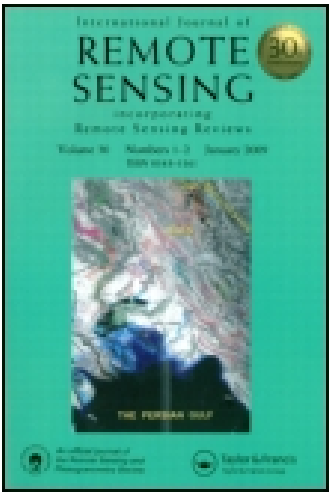

International Journal of Remote Sensing
Publication details, including instructions for authors and subscription information:
http://www.tandfonline.com/loi/tres20

Challenges of satellite rainfall estimation over mountainous and arid parts of east Africa

Tufa Dinku [a] , Pietro Ceccato [a] & Stephen J. Connor [a]
[a] International Research Institute for Climate and Society, The Earth Institute at Columbia University , 61 Route 9W, Palisades, NY, 10964, USA
Published online: 02 Aug 2011.

International Journal of Remote Sensing
Vol. 32, No. 21, 10 November 2011, 5965–5979

Taylor & Francis
Taylor & Francis Group

Challenges of satellite rainfall estimation over mountainous and arid parts of east Africa*

TUFA DINKU**, PIETRO CECCATO and STEPHEN J. CONNOR
International Research Institute for Climate and Society,
The Earth Institute at Columbia University, 61 Route 9W, Palisades, NY 10964, USA

(*Received 27 February 2009; in final form 14 September 2009*)

Different satellite rainfall products are used in different applications over different parts of the world. These products are particularly important over many parts of Africa, where they are used to augment the very sparse rain-gauge network. However, the quality of the different satellite products varies from one product to another and from one climatic region to another. The climate over eastern Africa varies from wet coastal and mountainous regions to dry arid regions. Significant variations could be observed within short distances. The different climates will pose different challenges to satellite rainfall retrieval over this region. This study explores the effect of mountainous and arid climates on four different satellite rainfall-estimation (RFE) algorithms. The mountainous climate is located over the Ethiopian highlands, while the arid region covers parts of Ethiopia, Djibouti and Somalia. One infrared-only product, African rainfall climatology (ARC), one passive-microwave-only product (the Climate Prediction Center morphing technique, CMORPH) and two products (the RFE algorithm and the tropical rainfall measuring mission (TRMM-3B42)), which combine both infrared and passive-microwave estimates, are used for this investigation. All the products exhibit moderate underestimation of rainfall over the highlands of Ethiopia, while the overestimation over the dry region is found to be very high. The underestimation over the mountainous region is ascribed to the warm orographic rain process, while the overestimation over the dry region may be because of sub-cloud evaporation. Local calibration of satellite algorithms and merging of satellite estimates with all locally available rain-gauge observations are some of the approaches that could be employed to alleviate these problems.

1. Introduction

The distribution of rain gauges over many parts of Africa is very sparse. In addition, the available stations are distributed unevenly, and most of the stations are located in cities along the major roads. The data from the cities may not represent what is

*This paper came from a workshop entitled '*Potentialities and Limitations in the Use of Remote Sensing for Detecting and Monitoring Environmental Change in the Horn of Africa*'. The workshop was organized by Somalia Water and Land Information Management (SWALIM) between 13 and 14 June 2007 at the Holiday Inn in Nairobi, Kenya. SWALIM is a project of the UN-FAO in Somalia (www.faoswalim.org).

**Corresponding author. Email: tufa@iri.columbia.edu

International Journal of Remote Sensing
ISSN 0143-1161 print/ISSN 1366-5901 online © 2011 Taylor & Francis
http://www.tandf.co.uk/journals
http://dx.doi.org/10.1080/01431161.2010.499381

going on away from the highways where the data is needed most. Satellite rainfall estimates are used to augment the gauge measurements. In fact, there are many parts of Africa where satellite products are the only sources of rainfall information. However, the quality of the satellite rainfall products is not very good, particularly at higher temporal and spatial resolutions. The quality also varies from one product to another, and from one climatic region to another. The climate over eastern Africa varies from arid lowlands to wetter highlands and coastal areas. The different climates have different implications on satellite rainfall-retrieval algorithms. This article investigates the effect of mountainous and arid regions on different satellite rainfall-estimation (RFE) algorithms.

The most widely used sensors for satellite RFE are thermal-infrared (TIR) and passive-microwave (PM) sensors. The information from TIR observation is mainly on the temperature of the top of a cloud, from which the depth of the cloud is inferred. PM sensors provide more information about precipitation because of the physical interaction between PM wavelengths and precipitation. However, currently, PM sensors are available only on board polar-orbiting satellites. This makes the observation frequency of PM sensors only a couple of times a day. As a result, current precipitation-retrieval algorithms use TIR, or a combination of TIR and PM. Both sensors have some serious limitations in retrieving rainfall, particularly over land (e.g. Levizzani *et al.* 2002, Gruber and Levizzani 2008, Wang *et al.* 2009). The limitations for TIR include the fact that it provides only information about the top of a cloud, underestimates warm rain and misidentifies cirrus clouds as raining. The main limitations for PM sensors include background emission from the land surface, which varies significantly depending on vegetation type and soil water content, low observation frequency (typically twice per day), which makes aggregation over daily time periods impossible, and beam-filling problems owing to the coarse spatial resolutions.

Mountainous and dry regions pose unique challenges to satellite rainfall retrievals, both from PM and TIR sensors. One challenge to TIR rainfall-retrieval algorithms comes mainly from warm orographic rains. Most TIR algorithms use fixed brightness-temperature thresholds to discriminate between raining and non-raining clouds. In addition, these thresholds are usually too cold for the warm orographic clouds, resulting in underestimation of rainfall. On the other hand, the rainfall signal for overland PM rainfall retrievals comes mainly from ice scattering at the upper parts of convective clouds. However, orographic rain may not produce much ice aloft, which may result in underestimation of surface rain. The other challenge to overland rain retrieval using PM algorithms comes from cold surfaces and ice over mountaintops, which could be misidentified as rain.

There are three main challenges to satellite rainfall retrieval over dry regions. The first one is sub-cloud evaporation. Over arid regions, the atmosphere beneath the clouds is mostly dry. As a result, although rainfall may be detected aloft, it will evaporate before reaching the surface resulting in huge overestimation of surface rainfall. The second challenge is a combination of the coarse spatial resolution of the satellite products (mostly about 0.25° latitude × 0.25° longitude) and the very hot background surface. The coarse-resolution image may cover both rain areas and hot surfaces whose average may be misidentified as a non-raining pixel. This may result in poor detection of surface rainfall. The third effect is specific to PM rainfall retrieval, and is related to a land-screening problem that identifies desert regions as raining (e.g. Wang *et al.* 2009).

To investigate the effects of highland and dry arid regions on rainfall retrieval from TIR and PM observations, four satellite rainfall products are evaluated over a mountainous region of Ethiopia and a dry region covering parts of Ethiopia, Djibouti and Somalia. The four satellite rainfall products are selected to enable the investigation of TIR-only, PM-only and combined TIR–PM algorithms. Thus, one of the products is the TIR-only product, the second is based mostly on PM estimates, and two of the products combine rainfall estimates from both TIR and PM sensors. The next section describes the study regions, the rain-gauge data used and the satellite products evaluated. Section 3 shows validation results, while section 4 discusses these results. Section 5 summarizes the findings.

2. Study region and data

2.1 *Study region*

Two validation sites with very different topography and climate were selected for this study. Both sites are located over the Horn of Africa (figure 1). The first site is located over the highlands of Ethiopia (S1 in figure 1). This site represents a complex

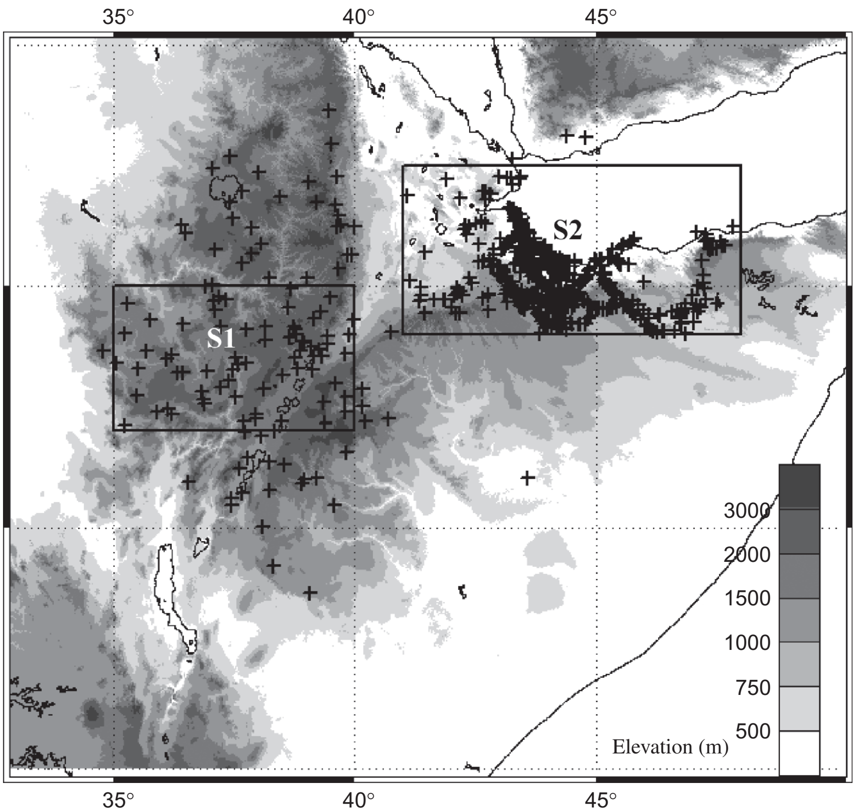

Figure 1. Topography and rain-gauge distribution of the validation sites. S1 represents a mountainous region, while S2 is an arid area. The plus (+) signs represent rain-gauge stations for S1 and its surrounding, and locations of field reports for S2.

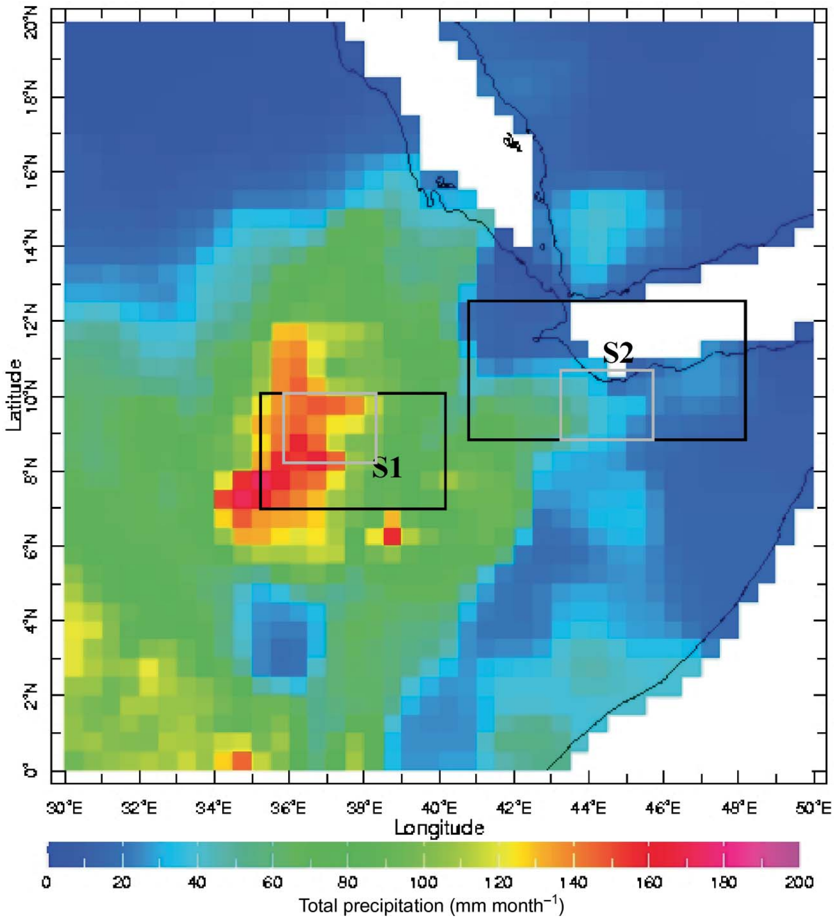

Figure 2. Mean (1971–1990) monthly rainfall. Boxes outlined with black show the validation sites, while boxes with grey outlines are used to compute area averages for the time series shown in figure 2. These data are obtained from the Global Precipitation Climatology Center (GPCC; Schneider *et al*. 2008), and they are the 'full data' products at a spatial resolution of 0.5°. The mean is limited to 1990 because there are no data over Somalia starting from 1991.

topography with significant variation in elevation from the rift valley in the centre to the mountains on either sides of the valley (figure 1). It is the wettest of the two validation sites (figures 2 and 3). The main rainy season is during June–September, but it also receives rainfall from February to October (figure 3). The main synoptic feature is the inter-tropical convergence zone (ITCZ); but its effect is very much modulated by the topography. The second validation site is a lowland area that covers parts of Ethiopia, Djibouti and Somalia (S2 in figure 1). It represents a relatively dry climate (figures 2 and 3). Its mean annual rainfall is about 30% of the wetter validation site. It has two rainy seasons, with peaks in April and August (figure 3). The two seasons are associated with north–south shifts of the ITCZ. These two sites represent very different climatic characteristics within a very close proximity. This will be shown to have different implications for satellite RFE algorithms.

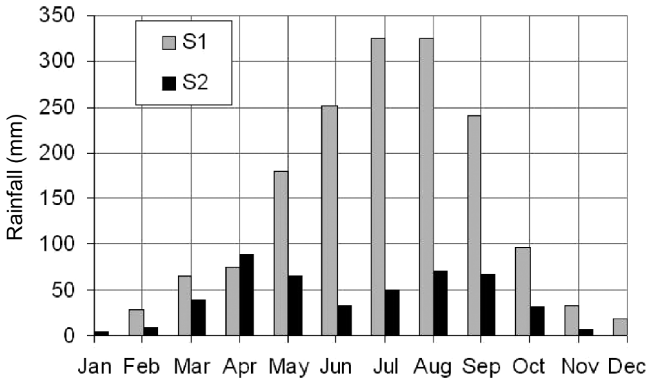

Figure 3. Mean (1971–1990) monthly rainfall averaged over the grey boxes in figure 2. S1 is for the site over the Ethiopian highlands, while S2 is for the arid region.

2.2 *Gauge data*

A relatively dense station network of about 140 gauges over the Ethiopian highland was used to evaluate the performance of different satellite products over a mountainous region. Out of the 140 stations, 75 fall within the area of interest (S1 in figure 1). Data from the summer months of 2003 and 2004 were used for the current analyses. These data were quality controlled and interpolated into regular grids using climatologically aided interpolation (Willmott and Robeson 1995). The climatological (mean) values were interpolated using kriging, while angular distance-weighted interpolation (New *et al.* 2000) was used to interpolate the anomalies. All available stations, except the few whose data is available through the global telecommunication system (GTS), were used in the interpolation. The GTS stations were excluded because they are incorporated in some of the products. However, only data within the validation box and with at least one gauge per pixel were used for validation.

The data used for the validation over the dry region (S2) were obtained from the Food and Agriculture Organization (FAO) of the United Nations. The FAO provided these data for the validation of satellite rainfall estimates over the desert locust recession regions, and S2 is one of those regions.

These are not rain-gauge measurements; rather, they are qualitative information collected during field campaigns by desert locust survey teams from the different member countries. Rainfall may be observed by the survey team itself, or the information may be collected from the locals. Sometimes the dates are precise, but often the timing and location could be vague. Here, the data were used only when the time and location of observation were reported to be exact. Figure 1 presents the different locations from where the reports were collected. The data for this box (S2) have not been interpolated because they are just binary (rain/no-rain) data from reports collected from *ad hoc* field campaigns. Thus, for each report, the closest satellite pixel is used for the comparisons. This means comparing a point measurement against an area average of a 10 km × 10 km or 25 km × 25 km pixel, and this would affect the result. This may also affect the comparison over the two validation sites, as the data over the first site have been interpolated. However, the spatial variability of rainfall over this region is relatively small and point-to-area comparison might not affect the result significantly.

2.3 *Satellite data*

Four satellite rainfall products are compared over the two validation sites. Three of the products come from the National Oceanic and Atmospheric Administration (NOAA) Climate Prediction Center (CPC). These include African rainfall climatology (ARC; Love *et al.* 2004), the African RFE algorithm (Herman *et al*. 1997, Xie *et al.* 2002) and the CPC morphing technique (CMORPH; Joyce *et al.* 2004). The fourth product is produced by the tropical rainfall measuring mission (TRMM) project at the National Aeronautics and Space Administration (NASA). The algorithm used is the TRMM multi-satellite precipitation analysis (TMPA; Huffman *et al.* 2007), and the product used here is TRMM-3B42. These products range from the simplest (ARC) to the most sophisticated (CMORPH), although it is not straightforward to compare TRMM-3B42 and CMORPH as they use different advanced algorithms. Table 1 provides summary information for these products.

The ARC is a TIR-only product adjusted with gauge data that are obtained through GTS. It is designed specifically to produce consistent high-resolution (0.1°) daily rainfall climatology for Africa. The objective was to produce daily rainfall time series starting from 1982, but the current available data starts from 1995. The NOAA CPC is working to produce the complete time series. The ARC algorithm uses a single TIR threshold (235 K) for the whole of Africa to discriminate between raining and non-raining clouds. This threshold is used to compute cold cloud duration (CCD) from 3-hourly TIR observations. Then, a single parameter is used to convert CCD into rain rates. The current version of the RFE algorithm, v. 2.0 (RFE2), is very similar to the ARC, except that it uses 0.5-hourly TIR observations and includes PM inputs (Xie *et al.* 2002). The previous version, v. 1.0 (RFE1; Herman *et al.* 1997), was operational from 1995 to 2000. RFE1 was a 10-daily product at 0.1° spatial resolution. There are two main differences between RFE1 and RFE2. The first is that RFE1 did not use PM inputs. The second difference is that RFE1 had a provision for taking orographic warm-rain processes into account, which is absent from the current version. The effect of orography was accommodated by combining relative humidity, wind direction and the terrain slope to estimate rainfall over regions where cloud-top temperatures are between 275 and 235 K.

The CMORPH algorithm is a new approach for combining PM rainfall estimates with TIR information. As such, CMORPH is not a RFE algorithm; rather, it is a technique whereby PM rainfall estimates, produced by different algorithms, are interpolated in space and time using motion vectors derived from 0.5-hourly TIR observations (Joyce *et al.* 2004). This algorithm starts with the time sequence of feature motions from the TIR data, and then this information is used to compute the displacement vector for morphing from one instantaneous microwave estimate to the

Table 1. Summary of the satellite products evaluated here.

	Time resolution	Space resolution	Existence	PM	Gauge
ARC	Daily	0.10°	1995–present	N	Y
RFE	Daily	0.10°	2000–present	Y	Y
TRMM-3B42	3 hourly	0.25°	1998–present	Y	Y
CMORPH	3 hourly	0.25°	2003–pressent	Y	N

Note: The PM and gauge columns indicate whether the product includes passive-microwave or gauge observations next. This enables CMORPH to combine the better RFE accuracy of PM estimates with TIR observations at higher temporal and special resolution. The final output from the CMORPH algorithm is still a PM-only product. Thus, here CMORPH is used to represent the PM-only products. The TMPA algorithm (Huffman *et al.* 2007) combines TIR data from geostationary satellites, PM data from different sources and GTS gauge reports. The TRMM-3B42 product is created in four steps: (1) the PM estimates are calibrated and combined, (2) TIR precipitation estimated are created using the PM estimates for calibration, (3) PM and TIR estimates are combined and (4) the data are rescaled to monthly totals whereby gauge observations are also used indirectly. TRMM-3B42 is a 3-hourly product at a spatial resolution of 0.25°.

3. Comparison of satellite rainfall products over mountainous and arid regions

Only the error statistic describing the rainfall detection capabilities of the satellite products is evaluated. This is because the FAO data is mainly qualitative and cannot reliably be used for evaluating the skill of the satellite products in estimating the amount of rainfall. The validation statistics used are frequency bias (FBS), probability of detection (POD), false alarm ratio (FAR) and Heidke skill score (HSS). The expressions for these statistics are given below. The expressions for the categorical statistics are also given below. These expressions are based on the contingency table (table 2), where A, B, C and D represent hits, false alarms, misses and correct negatives, respectively:

$$\mathrm{FBS} = \frac{A + B}{A + C} \tag{1}$$

$$\mathrm{POD} = \frac{A}{A + C} \tag{2}$$

$$\mathrm{FAR} = \frac{B}{A + B} \tag{3}$$

and

$$\mathrm{HSS} = \frac{2(AD - BC)}{(A + C)(C + D) + (A + B)(B + D)} \tag{4}$$

Table 2. Contingency table for comparing rain-gauge measurements and satellite rainfall estimates. The rainfall thresholds used are 1.0 and 0.5 mm, for the mountainous and dry region, respectively.

	Gauge $\geq$ threshold	Gauge $<$ threshold
Satellite $\geq$ threshold	A	B
Satellite $<$ threshold	C	D

The FBS compares the rainfall detection frequency of the satellite estimates with that of the rain gauge. It shows whether the satellite product underestimates (FBS < 1) or overestimates (FBS > 1) the rainfall events detected by the rain gauge. The POD assesses how good the satellite estimates are in detecting the occurrence of rainfall, while the FAR measures how often the satellite products detect rainfall when there is actually no rainfall. The HSS is a measure of the overall skill of the estimates accounting for matches due to random chance.

3.1 *Comparison of satellite rainfall products over the highland region*

Figure 4 compares the different validation statistics for the site over the Ethiopian highlands. The FBSs show that the satellite products underestimate the frequency of the rainfall. The POD is also low, except for CMORPH. All products have low FAR; that is, the problem of detecting rainfall when there is no rainfall is very small. Thus, the main problem over this region seems to be the moderate underestimation of the occurrence of rainfall.

Overall, the PM product (CMORPH) exhibits a relatively better performance, while the TIR-only product (ARC) has the poorest performance. The ARC has the highest underestimation of both amount and frequency of rainfall, while CMORPH has the lowest bias. CMORPH also has better rainfall detection (higher POD), while ARC has the poorest rainfall-detection statistics. Comparing the products that blend PM and TIR estimates, TRMM-3B42 shows a relatively better performance. This shows that single-threshold TIR products may not be suitable for such a mountainous region, while retrievals that make the best use of PM observations (CMORPH and TRMM-3B42) are better suited. The fact that ARC has relatively higher Correlation Coefficient (CC), with high underestimation and lower POD, means that the temperature threshold used is too low for this region. RFE uses the same threshold, but it also has PM input, which contributes to the improvement over ARC. The fact that RFE uses 30-minute TIR observations, while ARC uses 3-hourly observations may also contribute to the difference. The improvement of TRMM-3B42 over RFE comes mainly from the way PM inputs are used. In TRMM-3B42, the PM estimates are also used to calibrate the TIR brightness temperatures, while in RFE, the PM estimates are just combined with the TIR estimates. As a result, both the temperature thresholds and the

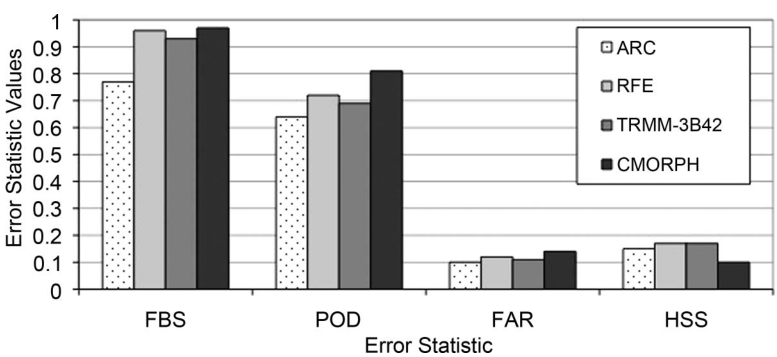

Figure 4. Comparison of satellite products for the mountainous region over Ethiopia (S1in figure 1). The number of points used to compute these statistics, $N = 1506$.

rain rate may vary from one location to the other in TRMM-3B42. The fixed temperature threshold and fixed rain rates are major shortcomings for the RFE algorithm. The improvement from TRMM-3B42 to CMORPH could be because the latter is totally based on PM estimates with TIR data used just to interpolate the PM estimates in time and space. As PM observations have a better physical relationship to precipitation, CMORPH appears to be doing better. It should also be noted that TRMM-3B42 uses gauge adjustments, while CMORPH does not. Thus, the better performance of CMORPH could be more significant than shown here.

3.2 *Comparison of satellite rainfall products over the arid region*

A comparison over the arid site is presented in figure 5. The FBS statistics show the opposite of what has been observed for the mountainous region. All the satellite products overestimate the frequency over the arid region, and the overestimation is very high. The overestimation of rain frequency is also reflected in the very high FAR values. On average, 87% rainfall detection by the satellite products is a false alarm. This is a serious problem for these satellite rainfall algorithms over this specific region. The FAR statistic is very sensitive to the climatology of the region, and the fact that rainfall is a rare event over this region may make this statistic less reliable. However, the fact that there is also high FBS lends some credibility to the FAR statistic. On the other hand, the POD is the only statistics that is comparable to that obtained for the mountainous region. The POD is also very low; the highest is 35% for RFE and the lowest is 22% for CMORPH. The HSS statistic shows that, although positive, the skills of the products in rainfall detection over this region are very low. The HSS values and hence the rainfall-detection skills, are much better over the highland region.

It is hard to decide which product performs better over this region. All products perform very poorly. RFE has slightly better POD, while TRMM-3B42 and CMORPH have lower FBS values. It is interesting to note that ARC, which uses a very simple algorithm, is as good as products from the more sophisticated algorithm. It is also curious why ARC seems to have slightly better FBS than RFE. One possible explanation for this could be the 3-hourly sampling frequency of the TIR data used in ARC compared to the 0.5-hourly sampling used for the other products. The low sampling frequency of ARC could reduce the overestimation of rainfall occurrence.

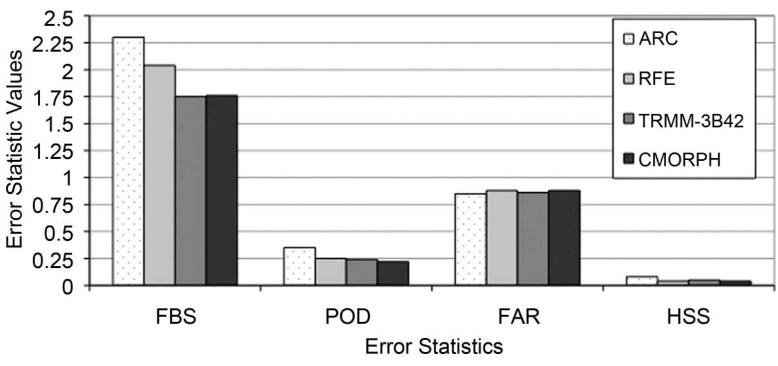

Figure 5. Same as figure 4, but for the arid region (S2 in figure 1). The number of points used to compute these statistics, $N = 1874$.

4. Discussion

The previous section presented the error statistics, which showed that the different satellite rainfall products have different problems over the different climatic regions studied here. There is some underestimation of rainfall frequency and amount over the mountainous region, while a huge overestimation is observed for the arid region. In this section, an attempt will be made to discuss the possible physical reasons behind those problems and how some of the problems may be alleviated.

4.1 *The mountainous region*

The underestimation over the highland region is mainly attributed to the complex orography and the associated warm-rain process. Products such as ARC and RFE use a single TIR threshold for discriminating between raining and non-raining clouds. However, this threshold could be too cold for regions where the warm-rain process dominates. Figure 6 shows temperature thresholds for discriminating raining and non-raining clouds over Ethiopia for the month of July. The suitable thresholds are different for the different parts of the country.

Note the difference between the thresholds for the southwestern and southern parts of the country. The threshold for the former region is relatively warm (−20°C), while it is much colder for the latter region (–60°C). Yet, the two regions are adjacent to each other. ARC and RFE will underestimate rainfall over the southwest region and

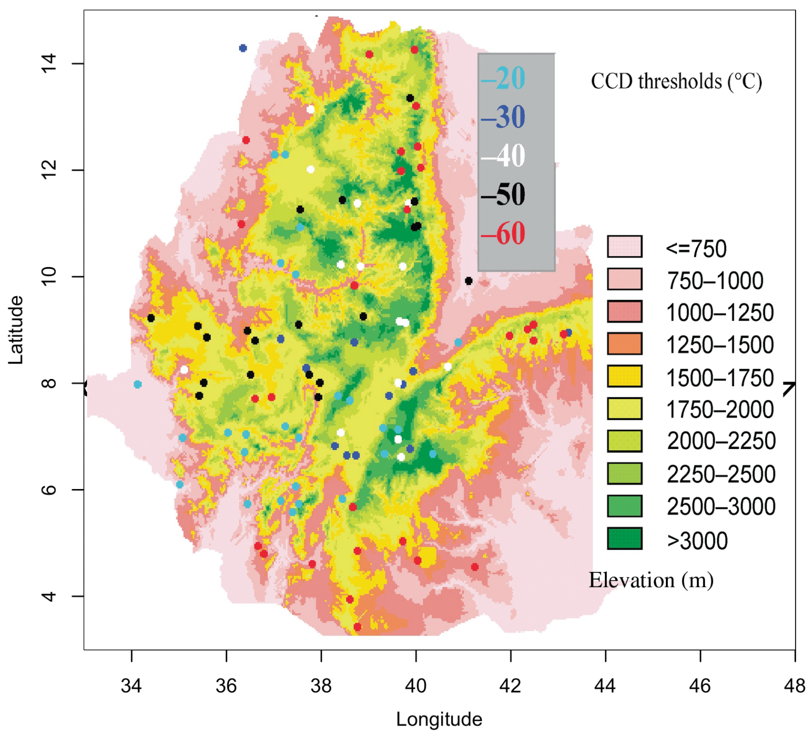

Figure 6. Distribution of suitable temperature thresholds (°C) for discriminating between rain and non-raining clouds for the month of July. The circles are locations of rain-gauge stations.

overestimate over the southern part. This is a result of the complex topography and synoptic features such as moisture sources. For PM rain retrieval, the main problem is that orographic rains may not produce much ice aloft. As current overland PM rainfall-retrieval algorithms depend on scattering by ice, this may lead to underestimation. Dinku *et al.* (2008) have shown the overall effect of orography on satellite RFE by comparing satellite products over Ethiopia and Zimbabwe. Most of Zimbabwe has a relatively flat topography; as a result, the performance of the products was much better. For example, correlation coefficients obtained for Zimbabwe were 0.64, 0.56 and 0.47 for RFE, TRMM-3B42 and CMORPH, respectively, compared with 0.26, 0.39 and 0.32 for Ethiopia.

4.2 *The arid region*

Section 3.2 showed the huge overestimation of rainfall frequency over the dry validation region by all the products. One major factor for this is perhaps sub-cloud evaporation. The atmosphere below the cloud is very dry over this region. As an example, figure 7 compares the long-term (1968–1996) mean relative humidity (%) over the two validation sites. The data comes from National Centers for Environmental Prediction (NCEP)/National Center for Atmospheric Research (NCAR) reanalysis (Kalnay *et al.* 1996). The left panel is for April and the right one for August. April and August are the months when the dry and mountainous regions, respectively, have their rainfall maxima (figure 3). Although the two validation boxes are very close to each other, the relative humidity over the two regions is drastically different. Relative humidity over S1 is above 80% during both months, while that over S2 is less than 60% even during the wettest month for the region. The effect of this dry atmosphere is that the rainfall detected aloft by the satellite sensors evaporates before reaching the ground. In addition, this may have resulted in the huge overestimation by the satellite algorithms. The other possibility, which is specific to PM algorithms, is that desert surfaces could be confused with rain signatures (e.g. Wang *et al.* 2009). This would obviously lead to overestimation.

4.3 *Tackling the problem*

The above discussions have described some of the challenges for satellite rainfall products over mountainous and arid regions. This does not mean that these are the only challenges, but they are the major ones for the current area of interest. The other challenge is over the coasts. Coastal effect is somewhat similar to that over the mountainous regions in that satellite rainfall products tend to underestimate rainfall. The question is how can we address these problems in the African context? One approach for taking orographic rain into account could be using the technique implemented in RFE1 (Herman *et al.* 1997). As discussed in section 2.3, the RFE1 algorithm has a module that takes orographic rainfall into account. As a result, RFE1 was found to be better than RFE2 over Ethiopia (Dinku *et al.* 2007). However, it might not be easy to implement this approach in the African context. In addition, this approach may not solve the major problem of the RFE algorithm, which is its use of a single temperature threshold.

Local calibration could be another approach. Figure 6 emphasizes the importance of local calibration. This figure shows the temperature that gives the smallest estimation error at station locations. It is obvious that different parts of the country need different TIR thresholds. The –60°C threshold works better for the southern

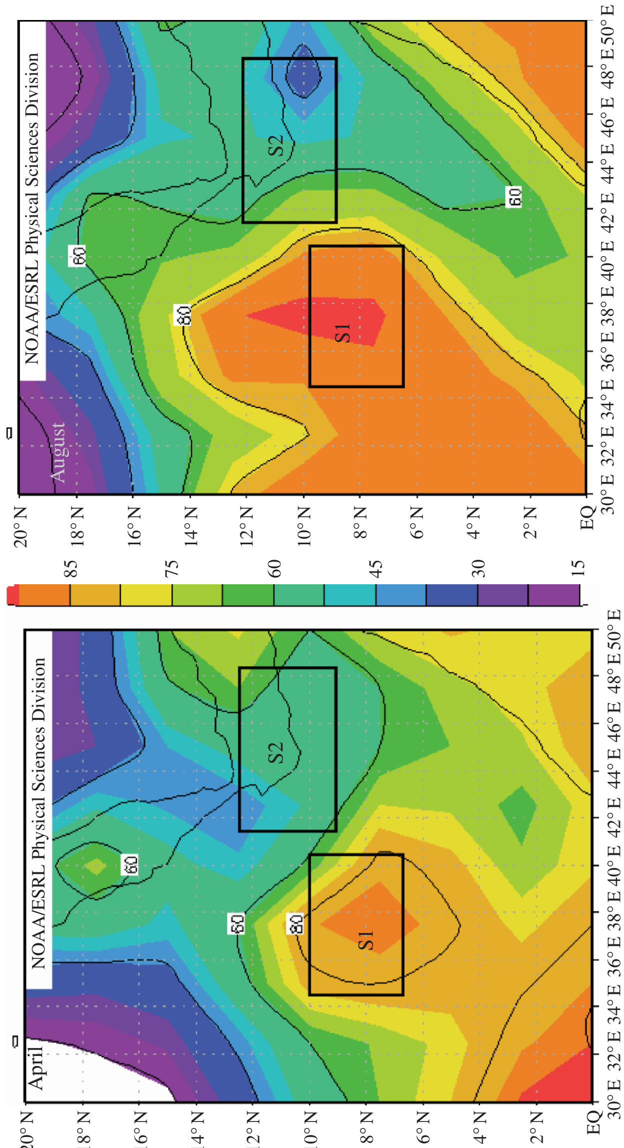

Figure 7. NCEP/NCAR reanalysis long-term (1968–1996) mean relative humidity (RH %) at 1000 mb for April (left) and August (right). The two rectangular boxes show the two validation sites. Image provided by the Physical Sciences Division, Earth System Research Laboratory, NOAA, Boulder, Colorado, from their web site at http://www.esrl.noaa.gov/psd/.

Table 3. Comparison of TAMSAT and CMORPH at 10-daily accumulation and 0.25° spatial resolution.

$N = 2448$	TAMSAT	CMORPH
CC	0.70	0.74
Eff	0.44	0.35
Bias	0.87	0.98
ME (mm)	−9	−1
RMS (%)	42	46

Notes: CC, Correlation Coefficient; Eff, Efficiency; ME, Mean Error; RMS, Root Mean Square Error.

and eastern parts of the country, –50°C could be better over some areas in the west, while −20°C might be needed for the southwestern parts. However, local calibration is not just a selection of appropriate temperature thresholds; it also involves determining the other relevant calibration parameters using local gauge observations. A good example that shows the value of local calibration is the tropical application of meteorology using the satellite data (TAMSAT) algorithm. This is a simple TIR-only algorithm, but uses different calibration parameters over different parts of Africa and different months (Grimes *et al.* 1999, Thorne *et al*. 2001). Table 3 compares the performance of the TAMSAT algorithm with that of CMORPH over Ethiopia. There is a big difference in the level of sophistication between the two algorithms; yet, TAMSAT performs as well as CMORPH. This is attributed to the specific calibration of the TAMSAT algorithm over Ethiopia. The problem with local calibration is that one needs access to rain-gauge data from the different countries. This has not been an easy task. Thus, the best approach could be helping individual countries in the region with calibration of the simple algorithms using their own rain-gauge data. Local calibration of sophisticated algorithms such as CMORPH may not be possible. However, the CMORPH, or other similar products, could be significantly improved by blending the products with rain-gauge observations. The blending process involves removing biases and then merging the satellite estimate with gauge observations. Of course, this process could also be used with the simpler algorithms. The blending process combines the point accuracy of the gauge observation with the better spatial coverage of the satellite products. This approach could now be used to generate about 30 years of better quality rainfall time series at higher temporal and spatial resolution.

5. Summary

The effect of highlands and arid regions on different satellite rainfall-retrieval algorithms has been investigated over eastern Africa. The algorithms investigated include simple algorithms (ARC and RFE) as well as the current state-of-the-art algorithms (CMORPH and TRMM-3B42). These products were evaluated using relatively dense rain-gauge observations from a mountainous region over Ethiopia and an arid region that covers parts of Ethiopia, Djibouti and Somalia. All satellite products moderately underestimated both the occurrence and amount of rainfall over the highland region. This underestimation was ascribed to the warm-rain process associated with the orography of the region. CMORPH was found to do better than the other products, while ARC exhibited the worst performance. The effect over the drier region is the exact opposite of that observed for the highland area. All the satellite rainfall products exhibited extreme overestimation of both frequency and amount of rainfall. The overestimation of the frequency of rainfall ranges between 175% for CMORPH to 230% for RFE. This extreme overestimation is mainly ascribed to evaporation of rainfall in the dry atmosphere under the cloud base.

The topography effect may be accounted for by using slope, moisture and wind data from numerical models, as was implemented in the previous version of RFE. However, local calibration could be another approach for the African context. Calibration that uses locally available rain-gauge observations could significantly improve RFE over the different climatic regions. This is better carried out by the countries themselves, as only a small fraction of gauge data is available outside the countries. Another approach to improving satellite rainfall products is combining the point accuracy of the gauge observations with the better spatial coverage of the satellite products. Satellite rainfall products now go back about 30 years. Thus, it is possible to produce good-quality and consistent historical time series by merging satellite estimates and gauge observations.

Acknowledgements
This work was funded by a grant/cooperative agreement from the NOAA, NA050AR4311004 and NASA HQ Science Mission Directorate Cooperative Agreement Notice NN-H-04-Z-YO-010-C through Cooperative Agreement # 06CR AG0028 with the US Geological Survey. The views expressed herein are those of the authors and do not necessarily reflect the views of NOAA, NASA or any of their sub-agencies. We are very grateful to the National Meteorological Agency of Ethiopia for providing us with all the rain-gauge data we requested, free of any charge. We also thank Keith Cressman of the FAO for providing part of the rainfall data used here.

References

Dinku, T., Ceccato, P., Grover-Kopec, E., Lemma, M., Connor, S.J. and Ropelewski, C.F., 2007, Validation of satellite rainfall products over east Africa's complex topography. *International Journal of Remote Sensing*, **28**, pp. 1503–1526.

Dinku, T., Chidzambwa, S., Ceccato, P., Connor, S.J. and Ropelewski, C.F., 2008, Validation of high-resolution satellite rainfall products over complex terrain in Africa. *International Journal of Remote Sensing*, **29**, pp. 4097–4110.

Grimes, D.I.F., Pardo, E. and Bonifacio, R., 1999, Optimal areal rainfall estimation using raingauges and satellite data. *Journal of Hydrology*, **222**, pp. 93–108.

Gruber, A. and Levizzani, V., 2008, Assessment of global precipitation products. WMO/TD-NO. 1430. Available online at: http://www.wmo.int/pages/prog/wcrp/documents/AssessmentGlobalPrecipitationReport.pdf (accessed 2 March 2011).

Herman, A., Kumar, V.B., Arkin, P.A. and Kousky, J.V., 1997, Objectively determined 10-day African rainfall estimates created for famine early warning. *International Journal of Remote Sensing*, **18**, pp. 2147–2159.

Huffman, G.J., Adler, R.F., Bolvin, D.T., Gu, G., Nelkin, E.J., Bowman, K.P., Hong, Y., Stocker, E.F. and Wolf, D.B., 2007, The TRMM multisatellite precipitation analysis (TMPA): quasi-global, multiyear, combined-sensor precipitation estimates at fine scales. *Journal of Hydrometeorology*, **8**, pp. 38–55.

Joyce, R.J., Janowiak, J.E., Arkin, P.A. and Xie, P., 2004, CMORPH: a method that produces global precipitation estimates from passive microwave and infrared data at high spatial and temporal resolution. *Journal of Hydrometeorology*, **5**, pp. 487–503.

Kalnay, E., Kanamitsu, M., Kistler, R., Collins, W., Deaven, D., Gandin, L., Iredell, M., Saha, S., White, G., Woollen, J., Zhu, Z., Leetmaa, A., Reynolds, B., Chelliah, M., Ebisuzaki, W., Higgins, W., Janowiak, J., Mo, K.C., Ropelewski, C., Wang, J., Jenne, R. and Joseph, D., 1996, The NCEP/NCAR 40-year reanalysis project. *Bulletin of the American Meteorological Society*, **77**, pp. 437–471.

Levizzani, V., Amorati, R. and Meneguzzo, F., 2002, A review of satellite-based rainfall estimation methods. Consiglio Nazionale delle Ricerche Istituto di Scienze dell'Atmosfera e del Clima. Available online at: http://www.geomin.unibo.it/hydro/music/reports/d6.1_satellite%20rainfall%20overview.pdf (accessed 2 March 2011).

Love, T.B., Kumar, V., Xie, P. and Thiaw, W., 2004, A 20-year daily Africa precipitation climatology using satellite and gauge data. In *Proceedings of the 84th AMS Annual Meeting, P5.4 in Conference on Applied Climatology*, 11–15 January 2004, Seattle, WA.

New, M.G., Hulme, M. and Jones, P.D., 2000, Representing twentieth-century space–time climate variability. Part II: development of 1901–1996 monthly grids of terrestrial surface climate. *Journal of Climate*, **13**, pp. 2217–2238.

Schneider, U., Fuchs, T., Meyer-Christoffer, A. and Rudolf, B., 2008, Global precipitation analysis products of the GPCC. Available online at: http://gpcc.dwd.de (accessed 2 March 2011).

Thorne, V., Coakeley, P., Grimes, D. and Dugdale, G., 2001, Comparison of TAMSAT and CPC rainfall estimates with raingauges, for southern Africa. *International Journal of Remote Sensing*, **22**, pp. 1951–1974.

Wang, N.-Y., Ferraro, R., Liu, C., Wolff, C.D., Zipser, E. and Kummerow, C., 2009, The TRMM 2A12 land precipitation product – status and future plans. *Journal of the Meteorological Society of Japan*, **87A**, pp. 237–253.

Willmott, C.J. and Robeson, S.M., 1995, Climatologically aided interpolation (CAI) of terrestrial air temperature. *International Journal of Climatology*, **15**, pp. 221–229.

Xie, P., Yarosh, Y., Love, T., Janowiak, J.E. and Arkin, P.A., 2002, A real-time daily precipitation analysis over south Asia. In *Preprints of the 16th Conference on Hydrology*, 12–17 January 2002 (Orlando, FL: American Meteorological Society).